AFCRL-68-0569

VORTEX INDUCED ROLLING MOMENTS ON FINNED MISSILES AT HIGH ANGLE OF ATTACK

by

Daniel G. Udelson

Engineering Laboratories
Boston University
110 Cummington Street
Boston, Massachusetts 02215

Contract No. F19628-68-C-0148
Project No. 7659
Task No. 765904
Work Unit No. 76590401

SCIENTIFIC REPORT No. 1

November 1968

Contract Monitor: Edward S. Mansfield
Aerospace Instrumentation Laboratory

Prepared
for

AIR FORCE CAMBRIDGE RESEARCH LABORATORIES
OFFICE OF AEROSPACE RESEARCH
UNITED STATES AIR FORCE
BEDFORD, MASSACHUSETTS 01730

55

AFCRL-68-0569

VORTEX INDUCED ROLLING MOMENTS ON FINNED MISSILES AT HIGH ANGLE OF ATTACK

by

Daniel G. Udelson

Engineering Laboratories
Boston University
110 Cummington Street
Boston, Massachusetts 02215

Contract No. F19628-68-C-0148
Project No. 7659
Task No. 765904
Work Unit No. 76590401

SCIENTIFIC REPORT No. 1

November 1968

Contract Monitor: Edward S. Mansfield
Aerospace Instrumentation Laboratory

Prepared
for

AIR FORCE CAMBRIDGE RESEARCH LABORATORIES
OFFICE OF AEROSPACE RESEARCH
UNITED STATES AIR FORCE
BEDFORD, MASSACHUSETTS 01730

ABSTRACT

Previous analytical studies endeavoring to account for vortex induced rolling moments on missiles have not successfully correlated with experimental results. This points up the need for a theoretically more sophisticated treatment, which the present work attempts to satisfy.

A model for the two dimensional cross flow past the tail body combination is employed and the Blasius complex contour integral used to find the moments. The integral is solved by examining the singularities (poles and branch points) inside the contour.

This is the first scientific report in a continuing research effort. The final result contained herein presents the complete mathematical solution for the two dimensional ideal flow past a planar tail body combination. It is in closed analytic form with the exception of one definite integral which has been reduced to a form suitable for numerical calculation. All terms of the solution (integrated as well as the integral) are best calculated for various values of the parameters on a large scale digital computer.

TABLE OF CONTENTS

LIST OF SYMBOLS

A	area
a	$\sqrt{c^2 - R^2}$
b	fin semi-span (see figures 3, 5 and 6)
c'	chord length
C_L'	sectional lift coefficient $\equiv \frac{L'}{q_\infty c}$
C_{M_0}'	sectional rolling moment coefficient $\equiv \frac{M_0'}{q_\infty b^2}$
C_{M_0}	rolling moment coefficient $\equiv \frac{M_0}{q_\infty L}$
C_N	normal force coefficient $\equiv \frac{N}{q_\infty A}$
c	$\frac{1}{2}\left(b + \frac{R^2}{b}\right)$ = radius of circle in the ζ plane (see Fig. 7 and 8)
C_Γ	vortex strength coefficient $\equiv \frac{\Gamma}{2\pi R v_\infty}$
$F(\zeta)$	$f(\zeta) w^2(\zeta)$
$f(\zeta)$	$z / \frac{dz}{d\zeta}$
$g(\zeta)$	see Appendix B
H	see Equ. (39)

List of Symbols (Continued)

$h(r)$	see Equ. (35)
$I^{m}_{\zeta_c}$	Blasius integral around pole of order m at ζ_0 (see Equ. (16))
$I_{I,II}$	Blasius integral around branch cut between ζ_I and ζ_{II}
i	unit pure imaginary number
L	length of fin (see Fig. 5)
L'	lift/unit length
ℓ	see Fig. 12
M	cross flow Mach number
M_o'	rolling moment/unit length of fin
M_o	rolling moment
m	order of pole
N	normal force on fin
q	dynamic pressure $= \frac{1}{2}\rho V_\infty^2$
R	radius of cylindrical body

List of Symbols (Continued)

r	polar coordinate (see Fig. 10)
S	line segment
U	cross flow velocity = $V_\infty \sin \alpha$
u	velocity in x direction or real component of velocity in the complex plane
V_∞	free stream velocity
V_t	tangential velocity of cylindrical surface due to roll
$\vec{V}$	vector velocity
v	velocity in y direction or imaginary component of velocity in the complex plane
v_n	component of vortex velocity normal to a fin surface
W	complex velocity potential
W_1	complex velocity potential in absence of the body
w	complex velocity = $u - iv$
X	fin axis in tail body plane (see Fig. 4 and 6)

List of Symbols (Continued)

η	axis perpendicular to x axis in tail body plane (see Fig. 4 and 6)
z	complex plane (see Fig. 6)
z'	complex plane of flat plate (see Fig. 7)
α	angle of attack of missile (see Fig. 5)
β	residue (see Equ. (15))
Γ	vortex strength
γ	arbitrary circulation around body
ϵ	radius of contour about branch point (see Fig. 10)
ζ	complex plane of the circle (see Fig. 8)
ζ_o	position of a pole in the ζ plane
$\zeta_I, \zeta_{II}, \cdots$	branch points in the ζ plane
$\eta(r)$	see Equ. (34)
θ	polar coordinate (see Fig. 10)
ρ	fluid density

List of Symbols (Continued)

φ	roll angle (see Fig. 4)
Ψ	stream function (imaginary part of W)

SECTION I. Introduction and Review of Previous Work

The successful research and development leading to modern rocket flight has brought with it several secondary aerodynamic problems to be solved as a result of the unstable behavior that these rockets occasionally exhibit. Some types of instability that have been experienced, in particular by sounding rockets, is caused by anomalous rolling moments which thus far have not been successfully predicted by theory.

Physical misalignments of the vehicle will tend to cause lack of symmetry about the roll axis. Hence the vehicle is usually made to spin by canting the fins, in order to minimize any non-symmetric behavior during flight through the atmosphere. In addition, spin provides a gyroscopic type stability in the endo-atmospheric environment. The roll rate is usually proportional to the rocket free stream velocity. However, as described in reference 1, disastrous results often occur when the roll rates deviate significantly from the expected values. For example, if the roll rate becomes the same as the natural pitching frequency of the vehicle, then pitch-roll coupling is liable to occur. That is, the rocket experiences the maximum angle of attack in the same plane; any misalignments tend to increase the angle of attack causing high drag in the atmosphere and high nutational movements outside of it.

Another type of instability is caused by the Magnus effect: due to spin there is a lateral force on the cylindrical body of the vehicle in a direction which is perpendicular to the angle of attack plane (i.e. the plane consisting of the free stream velocity vector and the body roll axis). (Ref. 2.) It may be shown that the roll induced force on the fins is in the opposite direction. (Ref. 3.) Thus, since the centers of pressure for the body and fins are separated,

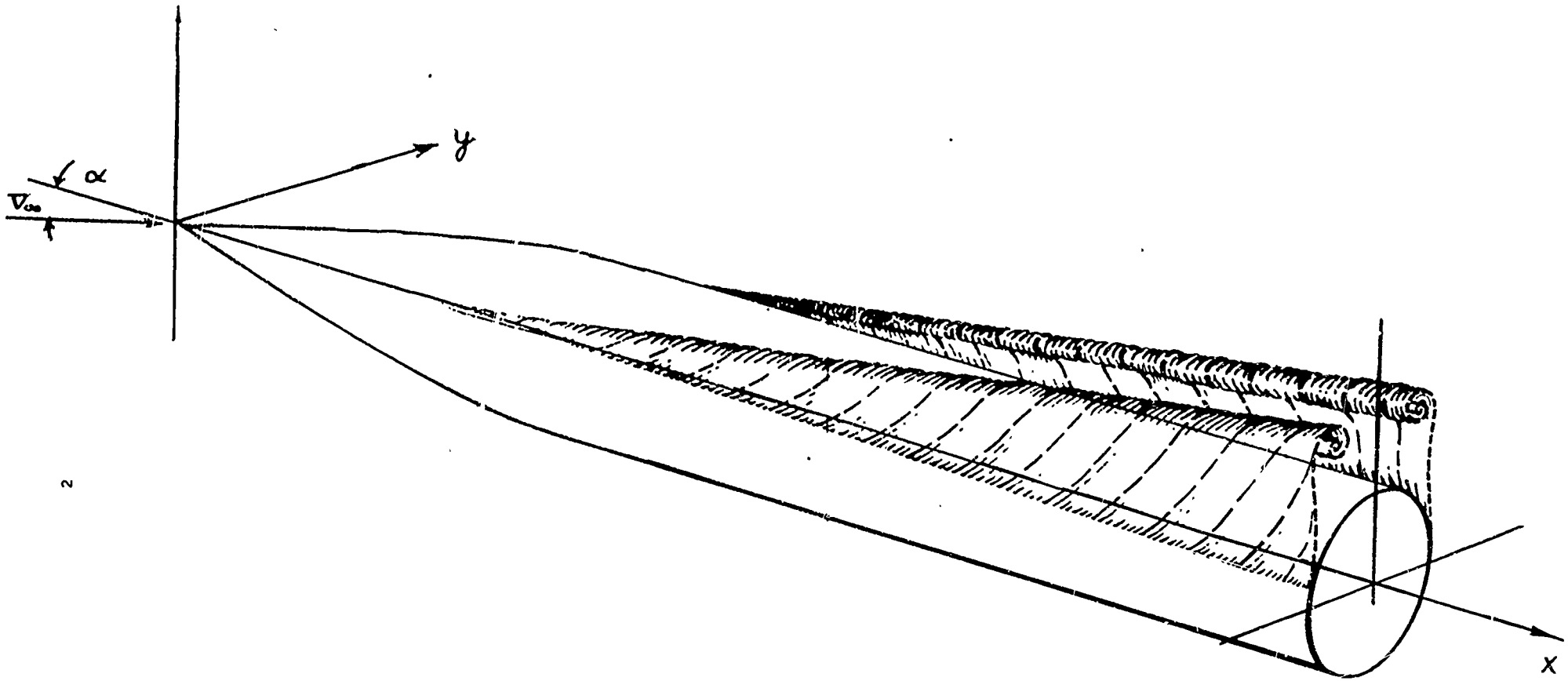

VORTEX GENERATION

Figure 1

there is a yawing moment on the vehicle. Needless to say, unpredictable roll rates (and therefore, to a large extent, uncontrollable roll rates) tend to aggrevate flight stability.

Many strange types of spin behavior have been experienced by reentry vehicles and torpedoes as well as rockets. These include spin reversal and constant velocity spin, even in cases where canted fins are part of the configuration. There have been several attempts in the literature to explain the unexpected rolling moments. For example, thermo-elastic effects on the fins, (Ref. 4), and oblique heat shield tape winding on the noses of reentry vehicles (Ref. 5) have accounted for small scale behavior, but have been heretofore unsuccessful in explaining some of the large moments that are observed. In particular, there is need for analytical work in the low roll case, as for sounding rockets where $V_t/V_\infty << 1$. (V_t is the tangential velocity of the cylindrical surface due to roll, and V_∞ is the free stream velocity.)

One approach that shows promise of explaining the rolling moment phenomena in the low roll case is as follows: at high angle of attack vortices are formed at the rear of the cylindrical body. When these vortices are shed, the longitudinal free stream velocity (the component along the body axis) washes them past the fins resulting in inteference that affects the rolling moment. Figure 1, which has been taken from Ref. 6, depicts the manner in which the vortices are formed on the non-finned part of the vehicle. Figure 2 (a), taken from Ref. 7, is a photograph in the cross flow plane. These vortices are symmetrical; however a roll velocity will cause non-symmetrical vortices as shown in Fig. 2 (b) (Ref. 7) for which $V_t / V_\infty = \frac{1}{2}$.

Fig. 2 (a)

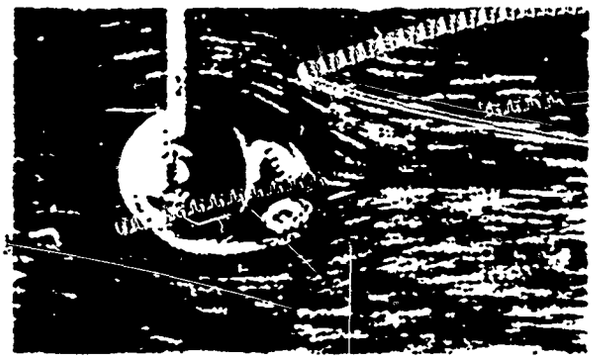

Fig. 2 (b)

Several attempts have been made in the literature to deal with vortex induced moments, but the analytical methods used have not been exact, and largely unsuccessful in predicting experimental results.

One approach (Ref. 6) uses the strip theory method: firstly

the flow in the cross plane is considered inviscid and incompressible (see Section II for a justification). Then potential fluid theory is employed to find the flow past a circular cylinder only, due to an external vortex, Γ , by suitably placing an image vortex inside the cylinder. A local angle of attack, α , on a fin as a function of the spanwise distance y (see Fig. 3) is described by dividing the velocity induced by the vortex normal

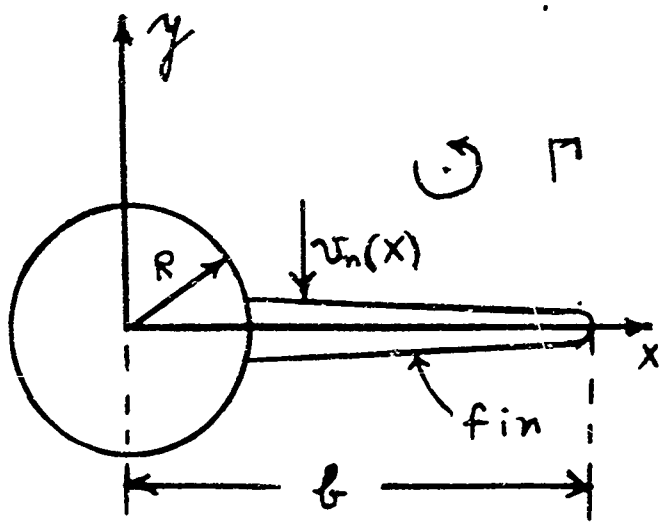

Fig. 3

to the fin surface, v_n , by the free stream velocity, V_∞ . Then the element of normal force on the fin is taken to be

$$dN = q C_{N_\alpha} \alpha(x) c(x) dx$$

where c is the chord length, q the dynamic pressure and, assuming linear theory,

$$C_{N_\alpha} \equiv \frac{dC_N}{d\alpha}$$

is the normal force coefficient slope. The rolling moment on one fin is given by

$$dM_o' = x\,dN$$

and thus

$$M_o' = \int_b^R q\, C_{N_\alpha} \frac{v_n}{V_\infty} x\, \alpha(x)\, dx .$$

The induced rolling moment on a multi-fin configuration is then obtained by addition.*

Rolling moments calculated by the preceeding method using symmetric vortices did not agree with those obtained from wind tunnel studies. (Ref. 6, p. 35) Obviously strip theory, although successful in some applications, has many shortcomings. First of all the streamlines due to a vortex in the presence of a cylinder only, is not the same if a fin is added; indeed, by the time the vortex reaches the fin, the streamlines are distorted so that there is no normal velocity component. To suppose that the normal force curve slope, C_{N_α}, on a flat plate caused by a true free stream angle of attack is the same as that due to the α defined above, is an approximation at best. Certainly a more accurate model would be to find the vortex flow in the presence of the fins as well as the cylinder. Secondly, even if the moment on one fin could be correctly computed, the total moment due to all the fins cannot be correctly obtained by addition, since each fin interferes with

---

*The appropriate flat plate coefficient for supersonic linear theory is (Ref. 8) $C_{N_\alpha} = \frac{4}{\sqrt{M_\infty^2 - 1}}$.

and obstructs the flow past the others. While strip theory might give good predictions of moment for a single fin in the vicinity of the vortex, multiple fins present a much too complicated flow field to be attacked by the simple model. Thirdly, the effect of the component of free stream velocity in the cross flow plane is not accounted for, nor is a possible Kutta condition in this plane considered.

Reference 9 is a continuation of the work of Ref. 6, and attempts to improve results. It uses a better expression for the normal force coefficient C_N by taking account of non-linear hypersonic terms; the expression is equivalent to

$$C_N = \frac{dC_N}{d\alpha}\alpha + \frac{1}{2}\frac{d^2C_N}{d\alpha^2}\alpha^2 + \cdots .$$

However, comparisons between experimental data and theory showed no improvement. (Ref. 9, p. 18.)

In Ref. 10 still another theoretical approach is presented; slender body theory is used in conjunction with the momentum method to get an order of magnitude estimate for rolling moments. However, one needs experimental values of the base pressures in order to apply the momentum method.

There have been attempts to find vortex induced moments experienced by varying cross sectional slender airplanes in unsteady flow using the Blasius method. (Ref. 11 and 12.) However, the correctness of this work is questionable. One of the shortcomings, among others, is the failure to account for the fact that Blasius' formula does not allow for varying cross-section in unsteady flow. (See Ref 13, p. 119.)

SECTION II. Formulation of the Problem

The general model which we would like to consider consists of inviscid flow past a long slender cylindrical body as depicted in Fig. 1, with a tail configuration as shown in Fig. 4. The cant of the fins is considered negligible, and the roll rate of the vehicle so low that steady state flow may be assumed.*

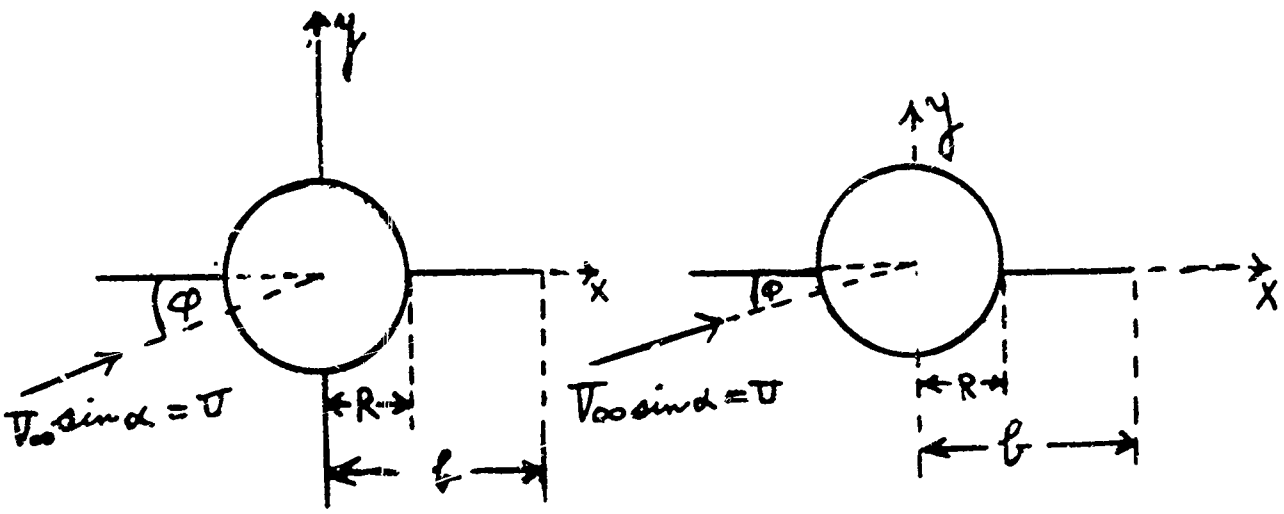

(a) Cruciform (b) Planar

Figure 4. Tail body configurations

Now consider the flow past the vehicle shown in Fig. 5.** It is assumed initially that the fins are rectangular flat plates

* The rolling moment to be found using these assumptions will be added to that due to fin cant, assuming that linearity allows for superposition.

** The effective angle of attack α is taken to include sideslip velocity.

(although the assumption of unvarying span can be relaxed as will be described in Section IV). The free stream velocity may be divided into the longitudinal component, $V_\infty \cos\alpha$, and the cross flow velocity $V_\infty \sin\alpha$. Because the fins are symmetrically placed and negligible roll is assumed, the longitudinal velocity component should have little effect on the rolling moment for non-canted fins. The force on any fin due to this component is

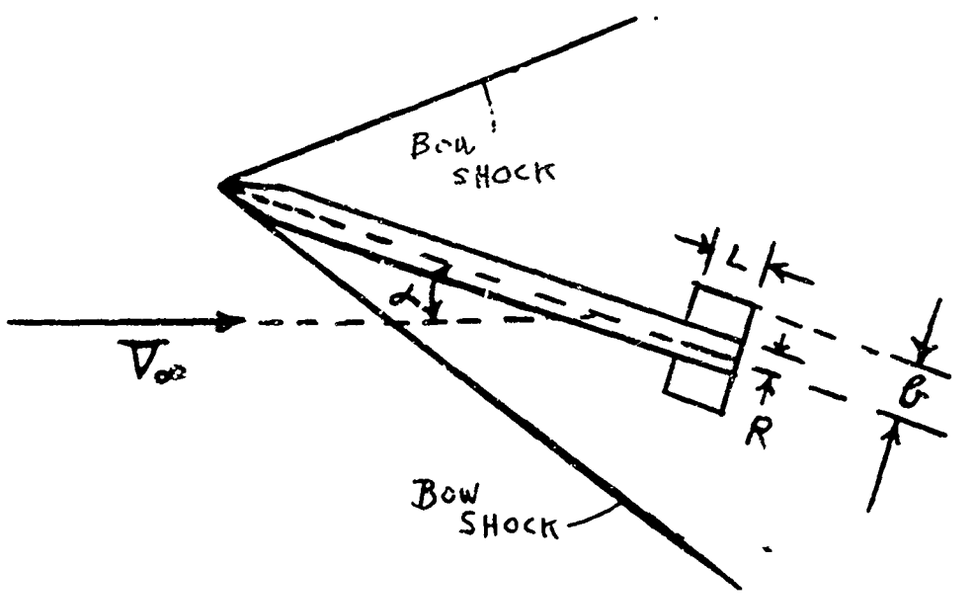

Figure 5

negated by the force on the opposing fin, 180° away. (Since the longitudinal flow is basically parallel to the long cylindrical surface it is unobstructed until it reaches each fin, and so should have the same effect on all.)*

* Naturally, the longitudinal flow will induce a moment on differentially canted fins.

On the other hand the cross flow velocity is a major factor in rolling moments. First of all it is the cause of the vortex generation and shedding depicted in Fig. 1. Secondly the cross flow should affect opposing fins differently since the cylindrical body presents an obstructive influence as the fluid goes past it. The main role of the longitudinal velocity is to wash the vortices produced on the main body surface aft, past the tail body combination.

For a typical free stream Mach number of 5 and an angle of attack equal to 20°, the cross flow Mach number is about 1.7. However, when we take the conical bow shock into consideration, (whose geometry is determined by the vehicle nose configuration), the cross flow velocity is further reduced, and must be subsonic in at least a considerable region behind the shock.

If one were interested in yawing or pitching moments, the entire body of the vehicle would play a role in the force distribution. Hence, since the vehicle contour changes in the longitudinal direction, a three dimensional treatment (usually approximated by slender body theory) would be called for. In the case of rolling moment, however, it is only the fins which experience contributing forces in inviscid flow, and since they are rectangular, the two dimensional cross flow problem will serve as our model. Because this flow has been shown to be largely subsonic, the approximation will be made that the cross flow Mach number is zero. It may later be necessary to use perturbation methods to take account of compressibility effects.

The final decision in describing the model is to choose the tail body configuration. Although the cruciform shape is common to the sounding rocket prototype, the ideal fluid which we have assumed would be questionable because flow separation is likely to

occur for any roll angle φ (see Fig. 4 (a)).* Moreover, the separated flow region is likely to be in the important vicinity of the shed vortices. Since a satisfactory mathematical model of separated flow phenomenon is lacking, we will choose our first physical model to be the planar tail body configuration (Fig. 4(b)). Then, at least for small roll angles, the question of separation is not as serious. Moreover, this model lends itself to taking account of compressibility effects by making a Prandtl-Glauert transformation, since the planar cross section obviously better satisfies the slender body requirement (for small φ) than does the cruciform configuration. Although the planar tail body does not represent the usual prototype it is a simplier mathematical model and one which is more consistent with the two dimensional physical reality. Our main purpose is to obtain an understadning of the fundamental phenomena underlying vortex induced moments. Once this understanding has been accomplished and successful correlations made with experiment, then it would be in order to attempt to formulate a model for flow past a cruciform tail as the next step.

Let U be the cross flow velocity, $V_\infty \sin \alpha$, past the configuration shown in Fig. 4 (b), reduced by an appropriate factor due to the conical bow shock wave.** The roll angle φ is the degree to which the fins have turned out of the vehicle's angle of attack plane. Let us represent the complex potential for this flow in the z plane by $W(z)$ (see Fig. 5) where account will be taken of two,

---

* The concern over separation is in a laboratory two dimensional experiment. In the rocket prototype, the longitudinal velocity component would largely eliminate any cross flow separation effects.

** U is assumed to be constant since the bow shock can be taken to be reasonably flat in the vicinity of the tail section.

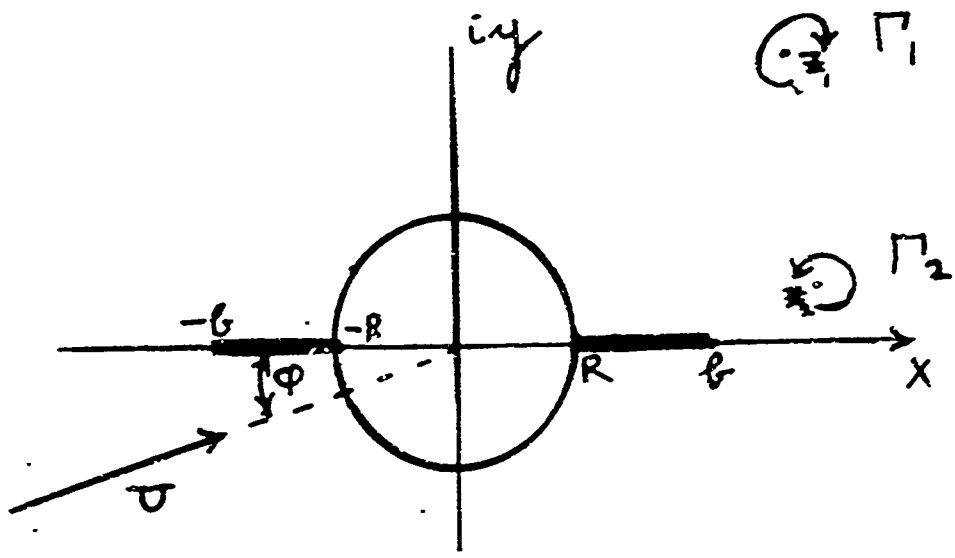

Figure 6. The z plane

not necessarily symmetrical vortices, Γ_1 and Γ_2.* Then the steady state rolling moment about the origin is given by the Blasius equation

$$(1) \quad M_o = -R_e \frac{\rho}{2} \oint z \left(\frac{dw}{dz}\right)^2 dz$$

where the contour is along the outside of the body surface. (Ref. 13, p. 49.)

It will be most expedient to evaluate Equ. (1) by mapping the body contour into a circle. This can be accomplished by a two step Joukowsky transformation:

$$(2) \quad z' = z + \frac{R^2}{z}$$

which maps the cross section into a flat plate (Fig. 7)

---

* It is clear that the strip theory method for finding the moments is no longer appropriate here since the velocity represented by $w = dW/dz$ has zero normal component to the fin surface.

and

$$(3) \quad z' = \zeta + \frac{c^2}{\zeta}$$

which maps the flat plate into a circle, (Fig. 8).

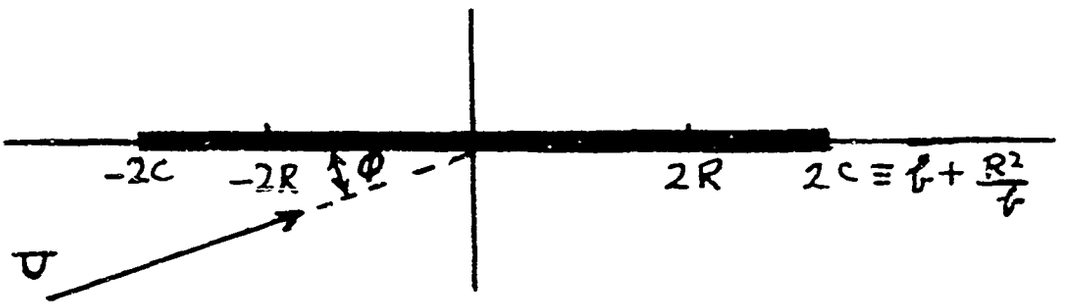

Figure 7. The z' plane

The points c and -c in the ζ plane are mappings of b- and $-b$ in the z plane. These transformations do not alter

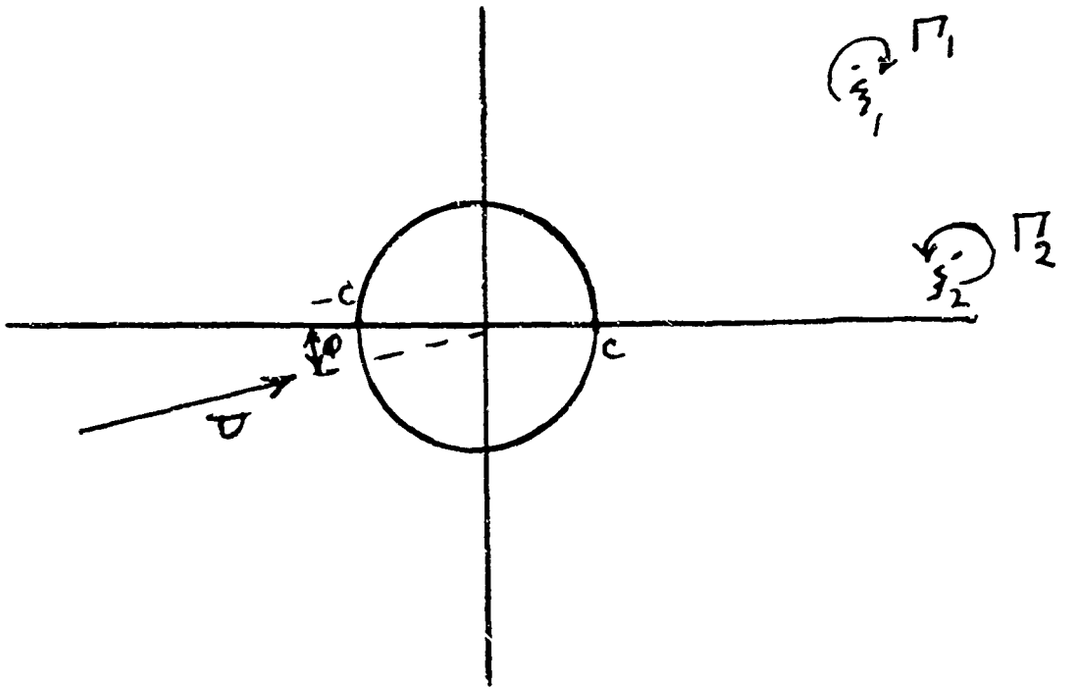

Figure 8. The ζ plane

the magnitude or direction of the free stream cross velocity, U, since (2) and (3) produce no distortions at infinity. Moreover, the vortex strengths Γ_1 and Γ_2 are the same in the z and ζ planes under these transformations. (See Appendix A for a proof.)

Combining (2) and (3) gives the direct relationships between z and ζ:

$$\text{(4a)}\quad \zeta = \frac{\left(z + \frac{R^2}{z}\right) + \sqrt{\left(z + \frac{R^2}{z}\right)^2 - 4c^2}}{2}$$

$$\text{(4b)}\quad z = \frac{\left(\zeta + \frac{c^2}{\zeta}\right) + \sqrt{\left(\zeta + \frac{c^2}{\zeta}\right)^2 - 4R^2}}{2}$$

where the choice of a positive rather than negative square root insures that the exterior of the body maps into the exterior of the circle.

The free stream complex potential in the ζ plane is $U e^{-i\varphi}\zeta$. Thus, if there are vortices of absolute strengths Γ_1 and Γ_2 located at ζ_1 and ζ_2 respectively, then the complex potential with no body present is

$$\text{(5)}\quad W_1(\zeta) = U e^{-i\varphi}\zeta + \frac{i\Gamma_1}{2\pi}\ln(\zeta - \zeta_1) - \frac{i\Gamma_2}{2\pi}\ln(\zeta - \zeta_2)$$

If we introduce a circle of radius c into the flow, the resulting complex potential is given by Milne-Thompson's Circle Theorem: (Ref. 14.)

$$\text{(6)}\quad W(\zeta) = W_1(\zeta) + \overline{W_1\left(\frac{c^2}{\zeta}\right)}$$

where the bar over an expression represents the complex conjugate

of that expression.* Substituting (5) into (6):

$$(7)\quad W(\zeta) = U e^{-i\varphi}\zeta + \frac{i\Gamma_1}{2\pi}\ln(\zeta-\zeta_1) - \frac{i\Gamma_2}{2\pi}\ln(\zeta-\zeta_2) + \overline{U e^{-i\varphi}\frac{c^2}{\zeta}} + \overline{\frac{i\Gamma_1}{2\pi}\ln\left(\frac{c^2}{\zeta}-\zeta_1\right)} - \overline{\frac{i\Gamma_2}{2\pi}\ln\left(\frac{c^2}{\zeta}-\zeta_2\right)}$$

This is not the unique solution for the flow in this problem. We can add a free vortex with center at the origin and arbitrary strength γ. We express its velocity potential in the form

$$\frac{i\gamma}{2\pi}\ln\frac{\zeta}{c}$$

whence the circle still remains a streamline (with $\Psi = 0$) and the velocity at infinity is not changed. This additional circulation around the origin will enable us to take account of a possible Kutta condition. Thus the velocity potential (7) can be supplemented and reduced as follows:

$$(8)\quad W(\zeta) = U\left(e^{-i\varphi}\zeta + e^{i\varphi}\frac{c^2}{\zeta}\right) + \frac{i\Gamma_1}{2\pi}\left[\ln(\zeta-\zeta_1) - \ln\left(\frac{c^2}{\zeta}-\bar{\zeta}_1\right)\right] - \frac{i\Gamma_2}{2\pi}\left[\ln(\zeta-\zeta_2) - \ln\left(\frac{c^2}{\zeta}-\bar{\zeta}_2\right)\right] + \frac{i\gamma}{2\pi}\ln\frac{\zeta}{c}.$$

To evaluate the Blasius integral in the ζ plane we note

---

* It can be easily shown that the imaginary part of (6) (the stream function) is zero on the circle, thus insuring that the circle is a streamline. Also $W(\infty) = W_1(\infty)$.

that $$\frac{dw}{dz} = \frac{dw}{d\zeta}\frac{d\zeta}{dz}$$

and therefore

$$(9) \quad w(z) = w(\zeta)\frac{d\zeta}{dz},$$

(where $w(z)$ and $w(\zeta)$ represent the complex velocities in the z and ζ planes respectively), or

$$w^2(z)dz = \frac{w^2(\zeta)}{dz/d\zeta}d\zeta.$$

Thus (1) becomes

$$M_o' = -Re\frac{\rho}{2}\oint z\frac{w^2(\zeta)}{dz/d\zeta}d\zeta$$

or

$$(10) \quad M_o' = -Re\frac{\rho}{2}\oint f(\zeta)w^2(\zeta)d\zeta$$

where

$$f(\zeta) \equiv \frac{z}{dz/d\zeta}$$

and the integral is evaluated along the circle $\zeta = C$. Using the expression for z as a function of ζ (Equ. (4b)) and its derivative

$$\frac{dz}{d\zeta} = \frac{1}{2}\left[1 - \frac{c^2}{\zeta^2} + \frac{\left(\zeta + \frac{c^2}{\zeta}\right)\left(1 - \frac{c^2}{\zeta^2}\right)}{\sqrt{\left(\zeta + \frac{c^2}{\zeta}\right)^2 - 4R^2}}\right]$$

gives, after considerable rearrangement,*

$$(11) \quad f(\zeta) = \frac{\zeta}{\zeta^2 - c^2}\left(\zeta^2 + c^2 - \frac{4R^2\zeta^2}{\sqrt{(\zeta^2+c^2)^2 - 4R^2\zeta^2} + (\zeta^2 + c^2)}\right)$$

Finally to evaluate (10), we need an expression for $w^2(\zeta)$; this is obtained by differentiating (8) and squaring:

$$(12) \quad W(\zeta) = \frac{dw}{d\zeta} = U\left(e^{-i\varphi} - e^{i\varphi}\frac{c^2}{\zeta^2}\right) + \frac{i\gamma}{2\pi\zeta}$$
$$+ \frac{i\Gamma_1}{2\pi}\left[\frac{1}{\zeta - \zeta_1} + \frac{1}{\zeta} - \frac{1}{\zeta - \frac{c^2}{\bar{\zeta}_1}}\right]$$
$$- \frac{i\Gamma_2}{2\pi}\left[\frac{1}{\zeta - \zeta_2} + \frac{1}{\zeta} - \frac{1}{\zeta - \frac{c^2}{\bar{\zeta}_2}}\right]$$

---

* See Appendix B for a tabulation of the derivatives of $f(\zeta)$.

and therefore

$$
\begin{aligned}
(13)\quad W'(\zeta) = \Bigg\{ & \bar{U}^2\left(e^{-2i\varphi} - \frac{2c^2}{\zeta^2} + e^{2i\varphi}\frac{c^4}{\zeta^4}\right) - \left(\frac{\gamma}{2\pi\zeta}\right)^2 \\
& - \left(\frac{\Gamma_1}{2\pi}\right)^2\left[\frac{1}{(\zeta-\zeta_1)^2} + \frac{1}{\zeta^2} + \frac{1}{\left(\zeta-\frac{c^2}{\bar{\zeta}_1}\right)^2} + \frac{2}{\zeta(\zeta-\zeta_1)}\right. \\
& \qquad \left. - \frac{2}{\zeta\left(\zeta-\frac{c^2}{\bar{\zeta}_1}\right)} - \frac{2}{(\zeta-\zeta_1)\left(\zeta-\frac{c^2}{\bar{\zeta}_1}\right)}\right] \\
& - \left(\frac{\Gamma_2}{2\pi}\right)^2\left[\frac{1}{(\zeta-\zeta_2)^2} + \frac{1}{\zeta^2} + \frac{1}{\left(\zeta-\frac{c^2}{\bar{\zeta}_2}\right)^2} + \frac{2}{\zeta(\zeta-\zeta_2)}\right. \\
& \qquad \left. - \frac{2}{\zeta\left(\zeta-\frac{c^2}{\bar{\zeta}_2}\right)} - \frac{2}{(\zeta-\zeta_2)\left(\zeta-\frac{c^2}{\bar{\zeta}_2}\right)}\right] \\
& + \frac{i\bar{U}\gamma}{\pi}\left[\frac{e^{-i\varphi}}{\zeta} - e^{i\varphi}\frac{c^2}{\zeta^3}\right] \\
& + \frac{i\bar{U}\Gamma_1}{\pi}\left[\frac{e^{-i\varphi}}{\zeta-\zeta_1} + \frac{e^{-i\varphi}}{\zeta} - \frac{e^{-i\varphi}}{\zeta-\frac{c^2}{\bar{\zeta}_1}}\right. \\
& \qquad \left. - \frac{e^{i\varphi}c^2}{\zeta^2(\zeta-\zeta_1)} - \frac{e^{i\varphi}c^2}{\zeta^3} + \frac{e^{i\varphi}c^2}{\zeta^2\left(\zeta-\frac{c^2}{\bar{\zeta}_1}\right)}\right] \\
& - \frac{i\bar{U}\Gamma_2}{\pi}\left[\frac{e^{-i\varphi}}{\zeta-\zeta_2} + \frac{e^{-i\varphi}}{\zeta} - \frac{e^{-i\varphi}}{\zeta-\frac{c^2}{\bar{\zeta}_2}}\right. \\
& \qquad \left. - \frac{e^{i\varphi}c^2}{\zeta^2(\zeta-\zeta_2)} - \frac{e^{i\varphi}c^2}{\zeta^3} + \frac{e^{i\varphi}c^2}{\zeta^2\left(\zeta-\frac{c^2}{\bar{\zeta}_2}\right)}\right] \\
& - \frac{\gamma\Gamma_1}{2\pi^2}\left[\frac{1}{\zeta(\zeta-\zeta_1)} + \frac{1}{\zeta^2} - \frac{1}{\zeta\left(\zeta-\frac{c^2}{\bar{\zeta}_1}\right)}\right] \\
& + \frac{\gamma\Gamma_2}{2\pi^2}\left[\frac{1}{\zeta(\zeta-\zeta_2)} + \frac{1}{\zeta^2} - \frac{1}{\zeta\left(\zeta-\frac{c^2}{\bar{\zeta}_2}\right)}\right] \\
& + \frac{\Gamma_1\Gamma_2}{2\pi^2}\left[\frac{1}{(\zeta-\zeta_1)(\zeta-\zeta_2)} + \frac{1}{\zeta(\zeta-\zeta_1)}\right. \\
& \qquad - \frac{1}{(\zeta-\zeta_1)\left(\zeta-\frac{c^2}{\bar{\zeta}_2}\right)} + \frac{1}{\zeta(\zeta-\zeta_2)} \\
& \qquad + \frac{1}{\zeta^2} - \frac{1}{\zeta\left(\zeta-\frac{c^2}{\bar{\zeta}_2}\right)} \\
& \qquad - \frac{1}{(\zeta-\zeta_2)\left(\zeta-\frac{c^2}{\bar{\zeta}_1}\right)} - \frac{1}{\zeta\left(\zeta-\frac{c^2}{\bar{\zeta}_1}\right)} \\
& \qquad \left. + \frac{1}{\left(\zeta-\frac{c^2}{\bar{\zeta}_1}\right)\left(\zeta-\frac{c^2}{\bar{\zeta}_2}\right)}\right]\Bigg\}
\end{aligned}
$$

Equation (10) is evaluated by deforming the contour and evaluating the integral around the singularities of $f(\zeta)w^2(\zeta)$.

From (13) we see that the singularities produced by $w^2(\zeta)$ are all poles, located at

$$\zeta = 0, \zeta_1, \zeta_2, \frac{c^2}{\bar{\zeta}_1} \quad \text{and} \quad \frac{c^2}{\bar{\zeta}_2}.$$

Since the vortices are located at ζ_1 and ζ_2, these points are exterior to the circle $\zeta = c$ and residues here do not contribute to the integral. On the other hand $|\zeta_1| > c$ guarantees that $\left|\frac{c^2}{\bar{\zeta}_1}\right| < c$, and thus the residues at $\zeta = \frac{c^2}{\bar{\zeta}_1}$ (and $\frac{c^2}{\bar{\zeta}_2}$) must be acccunted for.

The singularities of $f(\zeta)$ (Equ. (11)) all lie on the circle. They are poles at $\zeta = \pm c$ and branch points where the square root radical vanishes, that is where

$$(\zeta^2 + c^2)^2 - 4R^2\zeta^2 = 0$$

or

$$\zeta^2 + c^2 = \pm 2R\zeta.$$

Hence branch points are located where

$$\zeta^2 \pm 2R\zeta + c^2 = 0$$

or

$$\zeta = \pm R \pm i\sqrt{c^2 - R^2},$$

that is at the four points

$$(14)\qquad \begin{cases} \zeta_{I} = -R + ia & \zeta_{II} = R + ia \\ \zeta_{III} = R - ia & \zeta_{IV} = -R - ia \end{cases}$$

where

$$a \equiv \sqrt{c^2 - R^2}\ .$$

These are all obviously on the circle since in each case

$$|\zeta| = \sqrt{R^2 + a^2} = c.$$

SECTION III. Analytic Evaluation of the Contour Integral

If a complex function, $F(\zeta)$, has a pole of order m at $\zeta = \zeta_0$, then its residue there is (Ref. 15)

$$(15)\quad \beta = \lim_{\zeta \to \zeta_0} \frac{1}{(m-1)!} \frac{d^{(m-1)}}{d\zeta^{(m-1)}} \left[(\zeta - \zeta_0)^m F(\zeta) \right].$$

Thus, referring to Equ. (10), a contour around a pole with order m of the Blasius integral located at $\zeta = \zeta_0$ will be

$$(16)\quad I^m_{\zeta_0} = -\mathrm{Re}\, \pi i \rho \beta(\zeta_0, m)$$

where β is obtained by defining

$$(17)\quad F(\zeta) \equiv f'(\zeta) w^2(\zeta)$$

in Equ. (15).

The poles at $\zeta = c$ and $-c$ are simple ones. Thus at c, the integral is

$$I'_c = -\mathrm{Re}\, \pi i \rho \lim_{\zeta \to c} \left[(\zeta - c) \frac{\zeta w^2(\zeta)}{(\zeta - c)(\zeta + c)} \left(\zeta^2 + c^2 - \frac{4R^2\zeta^2}{(\zeta^2 + c^2)^2 - 4R^2\zeta^2 + (\zeta^2 + c^2)} \right) \right]$$

$$= -\mathrm{Re}\, \pi i \rho c \left[c - \frac{R^2}{a + c} \right] w^2(c).$$

Similarly, for the simple pole at $\zeta = -c$

$$I'_{-c} = -\mathrm{Re}\, \pi i \rho c \left[c - \frac{R^2}{a + c} \right] w^2(-c).$$

Thus the total contribution due to the poles at c and $-c$ is

$$(18)\quad I'_c + I'_{-c} = \mathrm{Re}\, \pi i \rho c \left[\frac{R^2}{a + c} - c \right] \left[w^2(c) + w^2(-c) \right].$$

Obviously, terms of $W^2(c)$ which are either real or odd will not contribute to this expression. Eliminating these terms from Equ. (13), substituting the remainder in (18), and combining terms gives, after considerable algebraic manipulation

$$
\begin{aligned}
(19)\quad I_c^{+} + I_{-c}^{-1} = \mathrm{Re}\, i\pi c\left[\frac{R^2}{a+c} - c\right]\Bigg\{ & -\frac{\Gamma_1^2}{\pi}\Bigg[\frac{c^2+\xi_1^2}{2(c^2-\xi_1^2)^2} \\
& + \frac{\bar{\xi}_1^2}{2c^2}\left(\frac{\bar{\xi}_1^2+c^2}{(c^2-\bar{\xi}_1^2)^2}\right) + \frac{1}{c^2-\xi_1^2} \\
& + \frac{1}{c^2}\left(\frac{\bar{\xi}_1^2}{c^2-\bar{\xi}_1^2}\right) + \bar{\xi}_1\left(\frac{\xi_1+\bar{\xi}_1}{(c^2-\xi_1^2)(c^2-\bar{\xi}_1^2)}\right)\Bigg] \\
& - \frac{\Gamma_2^2}{\pi}\Bigg[\frac{c^2+\xi_2^2}{2(c^2-\xi_2^2)^2} + \frac{\bar{\xi}_2^2}{2c^2}\left(\frac{\bar{\xi}_2^2+c^2}{(c^2-\bar{\xi}_2^2)^2}\right) \\
& + \frac{1}{c^2-\xi_2^2} + \frac{1}{c^2}\left(\frac{\bar{\xi}_2^2}{c^2-\bar{\xi}_2^2}\right) + \bar{\xi}_2\left(\frac{\xi_2+\bar{\xi}_2}{(c^2-\xi_2^2)(c^2-\bar{\xi}_2^2)}\right)\Bigg] \\
& + 4\sigma\Gamma_1 \sin\varphi\left(\frac{\xi_1}{c^2-\xi_1^2} + \frac{\bar{\xi}_1}{c^2-\bar{\xi}_1^2}\right) \\
& - 4\sigma\Gamma_2 \sin\varphi\left(\frac{\xi_2}{c^2-\xi_2^2} + \frac{\bar{\xi}_2}{c^2-\bar{\xi}_2^2}\right) \\
& - \frac{\gamma\Gamma_1}{\pi}\left[\frac{1}{c^2-\xi_1^2} + \frac{\bar{\xi}_1^2}{c^2}\left(\frac{1}{c^2-\bar{\xi}_1^2}\right)\right] \\
& + \frac{\gamma\Gamma_2}{\pi}\left[\frac{1}{c^2-\xi_2^2} + \frac{\bar{\xi}_2^2}{c^2}\left(\frac{1}{c^2-\bar{\xi}_2^2}\right)\right] \\
& + \frac{\Gamma_1\Gamma_2}{\pi}\Bigg[\frac{c^2+\xi_1\xi_2}{(c^2-\xi_1^2)(c^2-\xi_2^2)} + \frac{1}{c^2-\xi_1^2} \\
& + \bar{\xi}_2\left(\frac{\bar{\xi}_2+\xi_1}{(c^2-\xi_1^2)(c^2-\bar{\xi}_2^2)}\right) + \frac{1}{c^2-\xi_2^2} \\
& + \frac{\bar{\xi}_2^2}{c^2}\left(\frac{1}{c^2-\bar{\xi}_2^2}\right) + \bar{\xi}_1\left(\frac{\bar{\xi}_1+\xi_2}{(c^2-\xi_2^2)(c^2-\bar{\xi}_1^2)}\right) \\
& + \frac{\bar{\xi}_1^2}{c^2}\left(\frac{1}{c^2-\bar{\xi}_1^2}\right) + \frac{\bar{\xi}_1\bar{\xi}_2}{c^2}\frac{(c^2-\bar{\xi}_1\bar{\xi}_2)}{(c^2-\bar{\xi}_1^2)(c^2-\bar{\xi}_2^2)}\Bigg]\Bigg\}
\end{aligned}
$$

The contribution to the total moment due to the simple pole at $\zeta = 0$ is

$$I_0' = -\mathrm{Re}\,\pi i \left(\lim_{\zeta \to 0} \left\{ \zeta f(\zeta) \frac{1}{\zeta} \left[- \left(\frac{\Gamma_1}{2\pi}\right)^2 \left(\frac{2}{\zeta - \zeta_1} - \frac{2}{\zeta - \frac{c^2}{\zeta_1}} \right) + \cdots \right] \right\} \right.$$

where terms of $W^2(\zeta)$ (Equ. (13)) have been included which contain the factor $\frac{1}{\zeta}$. Obviously

$$I_0' = 0 \tag{20}$$

since $f(0) = 0$. (Equ. (11).)

To find the contribution of the second order poles at $\zeta = 0$, we use (16), (15) and (17):

$$\begin{aligned} I_0^2 = -\mathrm{Re}\,\pi i \left(\lim_{\zeta \to 0} \frac{d}{d\zeta} \left\{ \zeta^2 f(\zeta) \cdot \frac{1}{\zeta^2} \left[-2 v^2 c^2 \right.\right.\right. \\ - \left(\frac{\gamma}{2\pi}\right)^2 - \left(\frac{\Gamma_1}{2\pi}\right)^2 - \left(\frac{\Gamma_2}{2\pi}\right)^2 \\ + \frac{i v \Gamma_1 e^{i\varphi} c^2}{\pi} \left(- \frac{1}{\zeta - \zeta_1} + \frac{1}{\zeta - \frac{c^2}{\zeta_1}} \right) \\ - \frac{i v \Gamma_2 e^{i\varphi} c^2}{\pi} \left(- \frac{1}{\zeta - \zeta_2} + \frac{1}{\zeta - \frac{c^2}{\zeta_2}} \right) \\ \left.\left.\left. - \frac{1}{2\pi^2} \left(\gamma \Gamma_1 + \gamma \Gamma_2 + \Gamma_1 \Gamma_2 \right) \right] \right\} \end{aligned} \tag{21}$$

where terms of $W^2(\zeta)$ (Equ. (13)) have been included which contain the factor $\frac{1}{\zeta^2}$. Since

$$f(0) = 0 \quad \text{and} \quad f'(0) = -1$$

(see Appendix B), we have, differentiating (21), letting $\zeta = 0$,

collecting terms and eliminating pure imaginary numbers:

$$(22)\quad I_o^2 = -\mathrm{Re}\,\rho U e^{i\varphi}\left[\Gamma_1\left(\frac{c^2}{\xi_1}-\bar{\xi}_1\right)-\Gamma_2\left(\frac{c^2}{\xi_2}-\bar{\xi}_2\right)\right],$$

The contribution to the total moment due to the third order poles at $\xi = c$ is

$$I_o^3 = -\mathrm{Re}\,\pi i \rho \lim_{\xi\to c}\frac{1}{2}\frac{d^2}{d\xi^2}\left\{\xi^3 f'(\xi)\cdot\frac{1}{\xi^3}\left[-\frac{iU\gamma}{\pi}e^{i\varphi}c^2 - \frac{iU\Gamma_1}{\pi}e^{i\varphi}c^2 + \frac{iU\Gamma_2}{\pi}e^{i\varphi}c^2\right]\right\}$$

where terms of $w^2(\xi)$ have been included which contain the factor $1/\xi^3$. Hence

$$(23)\quad I_o^3 = \mathrm{Re}\,\frac{\rho U e^{i\varphi}c^2}{2}\left(-\gamma-\Gamma_1-\Gamma_2\right)f''(c) = 0$$

since $f''(0)=0$ (Appendix B).

The contribution to the total moment due to the fourth order poles at $\xi = c$ is

$$I_o^4 = -\mathrm{Re}\,\pi i\rho \lim_{\xi\to c}\frac{1}{6}\frac{d^3}{d\xi^3}\left[\xi^4 f'(\xi)\cdot\frac{1}{\xi^4}\left(U^2 e^{2i\varphi}c^4\right)\right]$$

where terms of $w'(\xi)$ have been included which contain the factor $\frac{1}{\xi^4}$.

Since $f'''(0)=\frac{12}{c^2}\left(\frac{R^2}{c^2}-1\right)$ (Appendix B),

$$I_o^4 = \mathrm{Re}\,2\pi\rho i U^2 e^{2i\varphi}\left(c^2-R^2\right)$$

or

$$(24)\quad I_o^4 = -2\rho\pi U^2\alpha^2\sin 2\varphi.$$

For the simple poles at $\xi = \frac{c^2}{\bar{\xi}_1}$, the contribution to the moment, again using (15), (16) and (17) is

$$I'_{c^2/\bar{\xi}_1} = -\mathrm{Re}\,\pi i \rho \lim_{\zeta \to \frac{c^2}{\bar{\xi}_1}} \left\{ \left(\zeta - \frac{c^2}{\bar{\xi}_1}\right) f(\zeta) \cdot \frac{1}{\left(\zeta - \frac{c^2}{\bar{\xi}_1}\right)} \right.$$

$$\cdot \left[-\left(\frac{\Gamma_1}{2\pi}\right)^2 \left(-\frac{2}{\zeta} - \frac{2}{\zeta - \xi_1}\right) + \frac{i\sigma\Gamma_1}{\pi}\left(-e^{-i\varphi} + \frac{e^{i\varphi} c^2}{\zeta^2}\right) \right.$$

$$\left. \left. + \frac{\sigma \cdot \Gamma_1}{2\pi^2} \frac{1}{\zeta} + \frac{\Gamma_1 \Gamma_2}{2\pi^2}\left(-\frac{1}{\zeta - \xi_2} - \frac{1}{\zeta} + \frac{1}{\zeta - \frac{c^2}{\bar{\xi}_2}}\right)\right]\right\}$$

where terms containing the factor $\frac{1}{\zeta - \frac{c^2}{\bar{\xi}_1}}$ in the expression for $w^2(\zeta)$ have been included. Thus

$$(25)\quad I'_{c^2/\bar{\xi}_1} = -\mathrm{Re}\,\Gamma_1 \rho i f\left(\frac{c^2}{\bar{\xi}_1}\right)\left[\frac{\Gamma_1 \bar{\xi}_1}{2\pi}\left(\frac{1}{c^2} + \frac{1}{c^2 - \xi_1 \bar{\xi}_1}\right)\right.$$

$$+ i\sigma\left(e^{i\varphi}\frac{\bar{\xi}_1^2}{c^2} - e^{-i\varphi}\right) + \frac{\sigma}{2\pi}\frac{\bar{\xi}_1}{c^2}$$

$$\left. - \frac{\Gamma_2 \bar{\xi}_1}{2\pi}\left(\frac{1}{c^2 - \bar{\xi}_1 \xi_2} + \frac{1}{c^2} - \frac{\bar{\xi}_2}{c^2(\bar{\xi}_2 - \bar{\xi}_1)}\right)\right]$$

where $f\left(\frac{c^2}{\bar{\xi}_1}\right)$ can be computed using Equ. (11). Similarly

$$(26)\quad I'_{c^2/\bar{\xi}_2} = -\mathrm{Re}\,\Gamma_2 \rho i f\left(\frac{c^2}{\bar{\xi}_2}\right)\left[\frac{\Gamma_2 \bar{\xi}_2}{2\pi}\left(\frac{1}{c^2} + \frac{1}{c^2 - \xi_2 \bar{\xi}_2}\right)\right.$$

$$+ i\sigma\left(e^{-i\varphi} - e^{i\varphi}\frac{\bar{\xi}_2^2}{c^2}\right) - \frac{\sigma}{2\pi}\frac{\bar{\xi}_2}{c^2}$$

$$\left. - \frac{\Gamma_1 \bar{\xi}_2}{2\pi}\left(\frac{1}{c^2 - \xi_1 \bar{\xi}_2} + \frac{1}{c^2} - \frac{\bar{\xi}_1}{c^2(\bar{\xi}_1 - \bar{\xi}_2)}\right)\right].$$

Finally, the remaining poles are second order ones at

$$\frac{c^2}{\bar{\xi}_1} \quad \text{and} \quad \frac{c^2}{\bar{\xi}_2} :$$

$$I^{2}_{c^2/\bar{\xi}_1} = -\,\mathrm{Re}\,\pi i \rho \lim_{\xi \to \frac{c^2}{\bar{\xi}_1}} \frac{d}{d\xi}\left[\left(\xi - \frac{c^2}{\bar{\xi}_1}\right)^2 f(\xi) \cdot \frac{-(\Gamma_1/2\pi)^2}{\left(\xi - \frac{c^2}{\bar{\xi}_1}\right)^2}\right]$$

$$= \mathrm{Re}\,\frac{i\Gamma_1^2 \rho}{4\pi} f'\left(\frac{c^2}{\bar{\xi}_1}\right).$$

By the same procedure

$$I^{2}_{c^2/\bar{\xi}_2} = \mathrm{Re}\,\frac{i\Gamma_2^2 \rho}{4\pi} f'\left(\frac{c^2}{\bar{\xi}_2}\right)$$

so that

$$(27)\quad I^{2}_{c^2/\bar{\xi}_1} + I^{2}_{c^2/\bar{\xi}_2} = \mathrm{Re}\,\frac{i\rho}{4\pi}\left[\Gamma_2^2 f'\left(\frac{c^2}{\bar{\xi}_2}\right) + \Gamma_1^2 f'\left(\frac{c^2}{\bar{\xi}_1}\right)\right]$$

with the expression for f' contained in Appendix B.

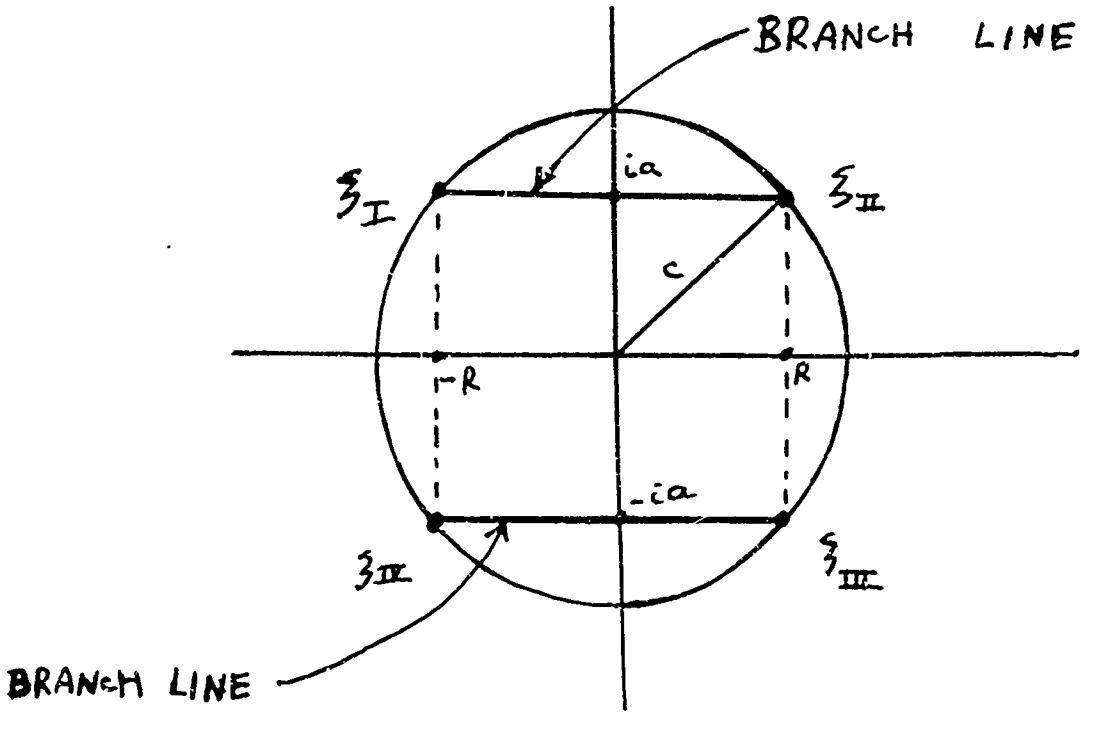

Fig. 9 Branch points and branch lines of $f(\xi)$

The remaining singularities where the contour integral must be evaluated are at the branch points ζ_I , ζ_{II} , ζ_{III}, and ζ_{IV} (see Equ. (14)). We arbitrarily choose as branch cuts the straight line segments joining ζ_I with ζ_{II} and ζ_{III} with ζ_{IV}, (Fig. 9).

The function $f(\zeta)$, which contains these square root singularities will be single valued and continuous as long as we move in the ζ plane without crossing the branch lines. Thus, for the integral enclosing points ζ_I and ζ_{II}, we choose the contour ABCDEFA, shown in Fig. 10, where CD and FA actually touch the branch line

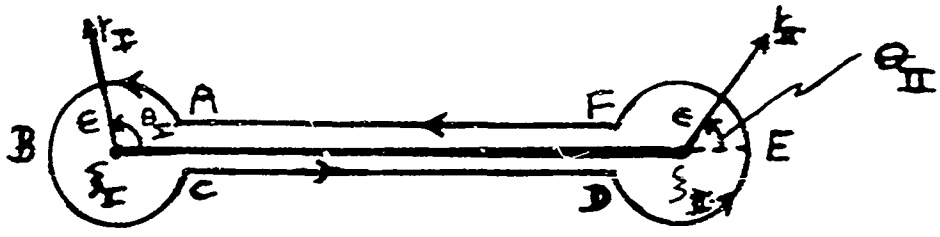

Fig. 10

but have been shown separated for visual purposes. ϵ will be allowed to approach zero. Referring to equations (10) and (11), the integral we wish to evaluate is

$$I_{I,II} = -\,Re\,\frac{f}{2}\int_{ABCDEFA}\frac{\zeta}{\zeta^2-c^2}\left[\frac{-4R^2\zeta^2 w'(\zeta)d\zeta}{\sqrt{(\zeta^2+c^2)^2-4R^2\zeta^2}+(\zeta^2+c^2)}\right]$$

or

$$(28)\quad I_{I,II} = Re\,2\rho R^2\int_{ABCDEFA}\frac{\zeta^5 w'(\zeta)d\zeta}{(\zeta^2-c^2)\left[\sqrt{(\zeta-\zeta_I)(\zeta-\zeta_{II})(\zeta-\zeta_{III})(\zeta-\zeta_{IV})}+\zeta^2+c^2\right]}$$

To evaluate the integrals around ABC and DEF we let $\zeta = \zeta_I + \epsilon e^{i\theta}$ and $\zeta = \zeta_{II} + \epsilon e^{i\theta}$ respectively, where θ is integrated between 0 and 2π in the first case, and between $-\pi$ and π in the second. If the integrand is denoted by $F(\zeta)$ then, for example,

$$\int_{ABC} F(\zeta)d\zeta = \int_c^{2\pi} F(\zeta_I + \epsilon e^{i\theta})\,i\epsilon e^{i\theta}d\theta .$$

It may be shown in general that if $\lim_{\zeta \to \zeta_I} \left| (\zeta - \zeta_I) F(\zeta) \right| = 0$ then the integral vanishes as $\epsilon \to 0$. This is indeed the case for the integrals ABC and DEF as may be varified by inspection. (See Appendix C for a proof of the theorem).

Now, considering the integrals along the lines FA and DC, we use the polar coordinates

$$r_I e^{i\theta_I} \equiv \zeta - \zeta_I \tag{29a}$$

$$r_{II} e^{i\theta_{II}} \equiv \zeta - \zeta_{II} \tag{29b}$$

where θ_I and θ_{II} are both allowed to vary between 0 and 2π (which automatically places the discontinuity along the designated branch cut.) On FA

$$\theta_I = 0 \quad \text{and} \quad \theta_{II} = \pi$$

while on CD

$$\theta_I = 2\pi \quad \text{and} \quad \theta_{II} = \pi$$

so that

$$\theta_I + \theta_{II} = \begin{cases} \pi & \text{on} \quad FA \\ 3\pi & \text{on} \quad CD \end{cases}$$

Hence

$$\sqrt{(\zeta - \zeta_I)(\zeta - \zeta_{II})} = \sqrt{r_I e^{i\theta_I} r_{II} e^{i\theta_{II}}}$$

$$= \sqrt{r_I r_{II}}\, e^{i(\theta_I + \theta_{II})/2}$$

$$= \begin{cases} \sqrt{r_I r_{II}}\, e^{i\pi/2} & \text{on} \quad FA \\ \sqrt{r_I r_{II}}\, e^{3\cdot\pi/2} & \text{on} \quad CD \end{cases}$$

or

$$(30)\quad \sqrt{(\xi-\xi_I)(\xi-\xi_{II})} = \begin{cases} i\sqrt{r_I r_{II}} & \text{on FA} \\ -i\sqrt{r_I r_{II}} & \text{on CD.} \end{cases}$$

Along FA, r_{II} varies between 0 and 2R as $\epsilon \to 0$ (see Fig. 9 and 10). Hence, using the substitution (29b):

$$\xi = \xi_{II} + r_{II} e^{i\theta_{II}}$$

$$= \xi_{II} + r_{II} e^{i\pi} \quad \text{on FA}$$

or

$$\xi = \xi_{II} - r_{II} \quad \text{and} \quad d\xi = -dr_{II}$$

on FA, and noting that

$$\xi - \xi_{III} = 2ia - r_{II}$$

and

$$\xi - \xi_{IV} \quad 2\xi_{II} - r_{II}$$

(see Equ. (14)), substitution of (30) into (28) gives

$$\int_{FA} = \mathrm{Re}\, 2\rho R^2 \int_0^{2R} \frac{(\xi_{II} - r_{II})^3 w^2 (\xi_{II} - r)(-dr_{II})}{\left[(\xi_{II} - r_{II})^2 - c^2\right]\left[i\sqrt{r_I r_{II}(2ia - r_{II})(2\xi_{II} - r_{II})} + (\xi_{II} - r_{II})^2 + c^2\right]}$$

Replacing r_I by $2R - r_{II}$, and dropping the subscript on r_{II} we have

$$(31)\quad \int_{FA} = -\mathrm{Re}\, 2\rho R^2 \int_0^{2R} \frac{(\xi_{II} - r)^3 w^2 (\xi_{II} - r)\, dr}{\left[(\xi_{II} - r)^2 - c^2\right]\left[i\sqrt{(2R-r) r (2ia - r)(2\xi_{II} - r)} + (\xi_{II} - r)^2 + c^2\right]}$$

Similarly, once more using the substitution (29b) in (28), r_{II} varies between 2R and 0 on CD while θ_{II} equals π, so that again

$$\xi = \xi_{II} - r_{II} \quad \text{and} \quad d\xi = -dr_I.$$

The only change in the integral is indicated by Equ. (30). Thus

dropping the subscript on r_{II} :

$$(32)\qquad \int_{CD} = -Re\, 2\rho R^2 \int_{2R}^{0} \frac{(\xi_{II}-r)^3 w^2(\xi_{II}-r)\,dr}{\left[(\xi_{II}-r)^2-c^2\right]\left[-i\sqrt{(2R-r)r(2ia-r)(2\xi_{II}-r)}+(\xi_{II}-r)^2+c^2\right]}$$

Adding (32) to (31), and after algebraic reduction, we obtain

$$(33)\qquad I_{\xi_I,\xi_{II}} = \int_{FA} + \int_{CD} = -Re\, 4i\rho R^2 \int_0^{2R} \frac{\eta^3 h(r) w^2(\eta)\,dr}{(\eta^2-c^2)\left[h^2(r)+(\eta^2+c^2)^2\right]}$$

where

$$(34)\qquad \eta(r) \equiv \xi_{II} - r = (R-r) + ia$$

and

$$(35)\qquad h(r) \equiv + \sqrt{(2R-r)\,r\,(2ia-r)(2R-r+2ia)}\ .$$

The same procedure is used for the integral around the branch cut connecting ξ_{III} with ξ_{IV} and produces

$$(36)\qquad I_{\xi_{III},\xi_{IV}} = -Re\, 4i\rho R^2 \int_0^{2R} \frac{\bar\eta^3\, \bar h(r) w^2(\bar\eta)\,dr}{(\bar\eta^2-c^2)\left[\bar h^2(r)+(\bar\eta^2+c^2)^2\right]}$$

with

$$\bar\eta(r) = \xi_{III} - r = (R-r) - ia$$

and

$$(37)\qquad \bar h(r) = \sqrt{(2R-r-2ia)(-2ia-r)\,r\,(2R-r)}\ .$$

It should be noted that the only difference between the integrands of (33) and (36) is in the sign of a.

We may combine (33) and (36):

$$(38)\quad I_{\xi_I,\xi_{II}} + I_{\xi_{III},\xi_{IV}} = -\mathrm{Re}\, 4i\rho R^2 \int_c^{2R} \left[H u^2(\eta) + \bar{H}\, w^2(\bar{\eta}) \right] dr$$

where

$$(39)\quad H \equiv \frac{\eta^3 h}{(\eta^2 - c^2)\left[h^2 + (\eta^2 + c^2)^2\right]} .$$

If we note that

$$\mathrm{Re}\, 4i\rho R^2 \int_c^{2R} \left[H w^2(\eta) + \bar{H}\, \bar{w}^2(\eta) \right] dr$$

$$= \mathrm{Re}\, 4i\rho R^2 \int_c^{2R} \mathrm{Re}\, H w^2(\eta)\, dr = 0$$

and add this result to (38), then the final expression is

$$(40)\quad I_{\xi_I,\xi_{II}} + I_{\xi_{III},\xi_{IV}} = \mathrm{Re}\, 4i\rho R^2 \int_c^{2R} \bar{H} \left[\bar{w}^2(\eta) - u^2(\bar{\eta}) \right] dr$$

with w^2 given by (13), H by (39), η by (34) and h by (35). Equation (40) is a definite proper integral of the real variable r (but with a complex integrand) and must have a finite value.

To summarize, the rolling moment given by the Blasius integral is the sum of the contour integrals around the singularities inside and on the circle $|\zeta| = c$ in the ζ plane. That is

$$(41)\quad M_c' = I_c' + I_{-c}' + I_0' + I_c^2 + I_{-c}^4$$

$$+ I'_{c^2/\bar{\xi}_1} + I'_{c^2/\bar{\xi}_2} + I^2_{c^2/\bar{\xi}_1} + I^2_{c^2/\bar{\xi}_2}$$

$$+ I_{\xi_I,\xi_{II}} + I_{\xi_{III},\xi_{IV}} .$$

The moment due to fin cant must be added to this result.* The equation for each of the integrals in (41) is listed in the table below:

Integral	Equ. number
$I_c^1 + I_{-c}^1$	(19)
$I_c^1 \equiv 0$	(20)
I_c^2	(22)
$I_c^3 \equiv 0$	(23)
I_c^4	(24)
I_{c^1/ξ_1}^1	(25)
I_{c^1/ξ_2}^1	(26)
$I_{c^1/\xi_1}^2 + I_{c^1/\xi_2}^2$	(27)
$I_{\xi_I, \xi_{II}} + I_{\xi_{III}, \xi_{IV}}$	(40)

The rolling moment, Equ. (41), can best be evaluated for various values of the parameters by use of a large scale digital computer. However, we can obtain results directly for special limiting cases. For example, consider the two dimensional flow, in the absence of external vortices, past a flat plate inclined at a roll angle (angle of attack) q with respect to the free

*See Section II and reference 3.

stream velocity, U . Obviously, since $R=0$ in Fig (4b), Equ. (40) indicates that

$$I_{\xi_I, \xi_{II}} + I_{\xi_{III}, \xi_{IV}} = 0.$$

Similarly, no external vortices in the flow means that $\Gamma_1 = \Gamma_2 = 0$; consequently, all the other integrals in Equ. (41) are clearly zero, with the exception of I_o^4. Thus, from (24)

$$M_o' = I_o^4 = -2\rho\pi U^2 a^2 \sin 2\varphi.$$

But for $R=c$

$$a = c = \frac{b}{2}.$$

Hence for a flat plate with no vortices

$$M_o' = -\frac{1}{2}\rho\pi U^2 b^2 \sin 2\varphi \qquad (42)$$
$$= -q b^2 \pi \sin 2\varphi$$

which is the well known moment about the center chord in ideal flow. In this case the lift L' acts at the quarter chord (aerodynamic center) so that

$$L'\frac{b}{2} = -M_o'$$

whence

$$C_{L'} \equiv \frac{L}{q(2b)} = -\frac{M_o'}{q b^2},$$

or using (42)

$$C_{L'} = \pi \sin 2\varphi$$

which becomes, for small angles

$$C_{L'} = 2\pi\varphi,$$

the classical result (see Ref. 16).

The other limiting case we will consider is that of a finless cylinder. Here $b = R$ (Fig. 4) so that

$$c = R \quad \text{and} \quad a = 0.$$

If there are no external vortices in the flow, $\Gamma_1 = \Gamma_2 = 0$ and

$$M_3' = I_0^4 + I_{\xi_I, \xi_{II}} + I_{\xi_{III}, \xi_{IV}}.$$

Since $a = 0$, Equ. (24) shows that

$$I_0^4 = 0.$$

Also, from (34)

$$\eta(r) = \bar{\eta}(r) = R - r \quad \text{(real)}$$

and from (35)

$$h(r) = +\sqrt{(2R-r)r(-r)(2R-r)}$$

$$= ir(2R-r).$$

Substituting these values into (39) gives

$$\bar{H} = \frac{-(R-r)^3 ir(2R-r)}{\left[(R-r)^2 - R^2\right]\left\{-r^2(2R-r)^2 + \left[(R-r)^2 + R^2\right]^2\right\}}$$

which is pure imaginary.

Moreover

$$\bar{w}^2(\eta) - w^2(\bar{\eta}) = \bar{w}^2(\eta) - w^2(\eta)$$

$$= -2 Q_m w^2(\eta).$$

Thus, Equ. (40) indicates that the integrand is the product of two imaginary variables, and is therefore real. Hence

$$I_{\xi_I, \xi_{II}} + I_{\xi_{III}, \xi_{IV}} = Re\ 4i\rho R^2 \int_0^{2R} (\text{Real variable})\, dr$$

$$= Re\ i\ (\text{Real number})$$

$$= 0$$

and so the rolling moment, M_o' , is zero for a finless cylinder, the expected result in ideal (frictionless) flow.*

*It is also expected that the rolling moment would be zero even in the presence of vortices, i.e., Γ_1 and Γ_2 not zero. In this case, since $C=R$, $a=0$ and $f(\zeta)=\zeta$, it can be shown that Equ. (19) and (27) both vanish while Equ. (22) cancels (25) and (26) so that, indeed, $M_o' = 0$.

SECTION IV Conclusion and Plans for Future Work

An analytical expression for the sectional moment rolling coefficient, M_o', has been found as a function of the following variables:

$$M_o' = M_o'(b, R, \zeta_1, \zeta_2, \Gamma_1, \Gamma_2, \rho, U, \varphi, \gamma).$$

There are, in fact, twelve independent variables since ζ_1 and ζ_2 are complex numbers, each consisting of two components. We may eliminate three parameters if we express the variables in dimensionless form:

$$(43)\quad \frac{M_o'}{\frac{1}{2}\rho U^2 b^2} \equiv C_{M_o'}\left(\frac{R}{b}, \frac{\zeta_1}{R}, \frac{\zeta_2}{R}, C_{\Gamma_1}, C_{\Gamma_2}, \varphi, \frac{\gamma}{2\pi R U}\right)$$

where $C_\Gamma \equiv \Gamma / 2\pi R U$

is defined as the vortex strength coefficient. It should be noted that

$$C \leq \frac{R}{b} \leq 1$$

where the extremes $\frac{R}{b} = C$ is for a flat plate and $\frac{R}{b} = 1$ is for a finless cylinder. The numerical data obtained from a computer will be most conveniently plotted using (43).*

As an example, we suppose that γ is determined by a Kutta condition and so need not be specified independently. For vortices fixed at ζ_1 and ζ_2, we may plot series of graphs with $C_{M_o'}$ as ordinate, φ as abscissa and $\frac{R}{b}$ as parameter, where each graph is for a pair of values C_{Γ_1} and C_{Γ_2}. Thus for the case $\Gamma_1 = \Gamma_2 = C$ we have, from

---

* The variables R and b are defined in the physical plane (see Fig. 4). If the location of the vortices are at z_1 and z_2 in the physical plane, their locations in the ζ plane may be determined from Equ. (4a). It will also be recalled that U, φ and Γ suffer no change in the transformation.

(42), for a flat plate

$$C_{M_0'} = -\pi \sin 2\Phi \qquad \left(\frac{R}{b} = 0\right)$$

while for a finless cylinder, there is no rolling moment in frictionless flow so

$$C_{M_c'} = 0 \qquad \left(\frac{R}{b} = 1\right).$$

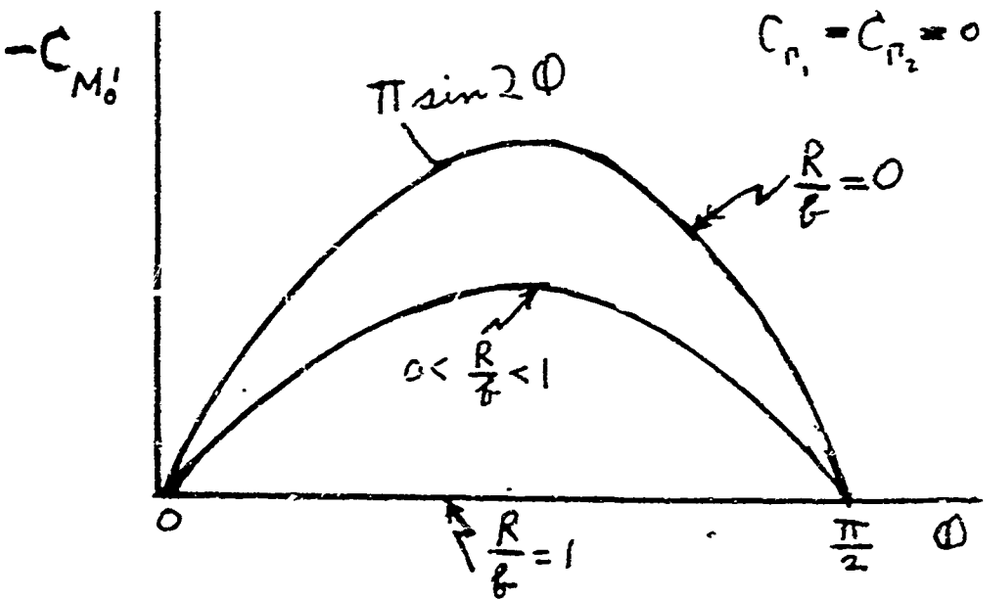

Fig. 11

The analysis in this report assumes a two dimensional fin. However if the fin is not rectangular, but has varying span b, we may integrate the sectional rolling moment M_0' in steady flow to find the total moment

$$M_0 = \int_0^L M_0' \, dl$$

where M_0' is a function of $b(l)$ and L is the fin length. (See Fig. 12). Then in Equ. (43) we may replace the dimensionless variable $C_{M_0'}$ by

$$C_{M_0} \equiv \frac{M_0}{\frac{1}{2}\rho U^2 L}$$

and $\frac{R}{b}$ by $\frac{R}{L}$.

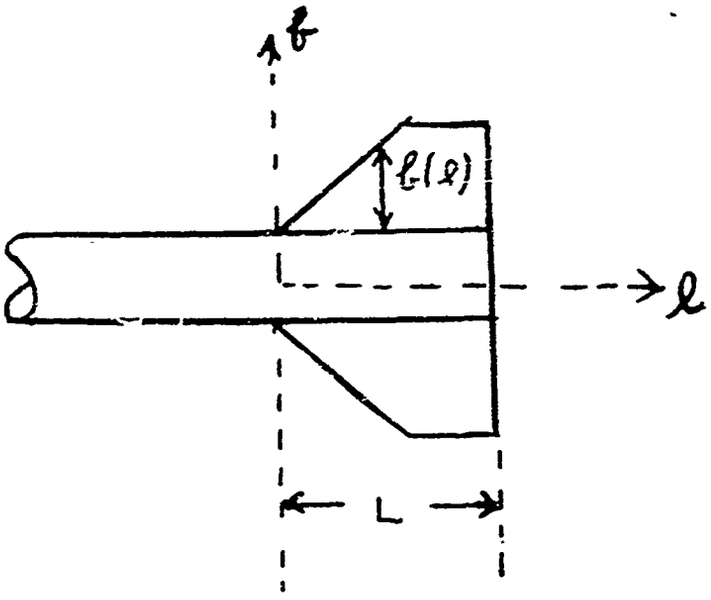

Fig. 12

In conclusion it is to be noted that this report is the first in a continuing research effort. The immediate future task is to obtain numerical results for the present analytical study. As another important undertaking it will be useful to extend this work to missiles with a cruciform tail body configuration. Also compressible and non-steady flow effects should be considered. Finally meaningful experiments should be devised and carried out to supplement the analysis.

REFERENCES

1. Mansfield, Edward, M.S. Thesis, College of Engineering, Boston Univ., Spring 1968.

2. Goldstein, S., "Modern Developments in Fluid Mechanics", Oxford Univ. Press, 1938.

3. Platou, Anders S., "Magnus Characteristics of Finned and Nonfinned Projectiles", AIAA Jour., Jan. 1965, p. 83.

4. Maun, E.K. "NIRO Vehicle Dynamic Analysis", SGC 497R-3, Space-General Corp., Jan. 1965.

5. Unpublished presentation of Avco MSD group at AIAA Aerospace Sciences Meeting, New York, Jan. 1968.

6. Perla, A., "On Induced Rolling Moments at High Angle of Attack", AFCRL Report, 1963.

7. Prandtl and Tietjens, "Applied Hydro and Aeromechanics", Dover Publications, 1957, p.279 and 286.

8. Kuethe and Schetzer, "Foundations of Aerodynamics", John Wiley and Sons, 1959, p.218.

9. J.P. Taylor, "NIRO Induced Rolling Moment Characteristics", Space-General Corp. Scientific Report to AFCRL No. SGC 497R-8, March, 1965.

10. Neilsen, J.N., "Missle Aeordynamics", McGraw Hill, 1960.

11. Sacks, A.H., "Aeordynamic Forces, Moments, and Stability Derivatives for Slender Bodies of General Cross Sction", NACA TN 3283, Nov., 1954.

12. Sacks. A.H. "Vortex Inteference on Slender Airplanes", NACA TN 3525, Nov. 1955.

13. Ashley and Landahl, "Aeordynamics of Wings and Bodies", Addison Wesley, 1965.

14. Milne-Thompson, "Theoretical Hydrodynamics", 2nd Ed., Macmillan Co., 1950, p. 149.

15. Churchill, R.V., "Introduction to Complex Variables and Applications", McGraw Hill, 1948, p. 121.

16. Von Mises, R., "Theory of Flight", Dover Publications, 1958, Sect. VIII. 2.

APPENDIX A

It will be proved here that a vortex undergoes no change in strength, Γ, under a conformal transformation from the z to ζ planes. By definition:

$$\Gamma = -\oint \vec{V} \cdot d\vec{s} = -\oint (u\,dx + v\,dy)$$

where the integral is evaluated counterclockwise in a curve enclosing the vortex.* Now, in the complex z plane

$$\begin{aligned} w(z)\,dz &= (u - iv)(dx + i\,dy) \\ &= (u\,dx + v\,dy) + i(u\,dy - v\,dx) \end{aligned}$$

so that

$$(\Gamma)_{z \text{ plane}} = -\operatorname{Re} \oint w(z)\,dz .$$

Similarly, in the ζ plane

$$(\Gamma)_{\zeta \text{ plane}} = -\operatorname{Re} \oint w(\zeta)\,d\zeta .$$

But by Equ. (9)

$$w(z)\,dz = w(\zeta)\,d\zeta .$$

Hence it follows that

$$(\Gamma)_{z \text{ plane}} = (\Gamma)_{\zeta \text{ plane}} .$$

---

* The negative sign is due to the fact that a positive circulation is, by convention, defined to be in the clockwise direction.

APPENDIX B

For reference purposes, the derivatives of $f(\xi)$ are listed here. From Equ. (11)

$$f(\xi) = \frac{\xi}{\xi^2 - c^2} \cdot g(\xi)$$

where

$$g(\xi) \equiv \xi^2 + c^2 - \frac{4R^2\xi^2}{\sqrt{(\xi^2+c^2)^2 - 4R^2\xi^2} + (\xi^2+c^2)}$$

Hence

$$f'(\xi) = -\frac{c^2+\xi^2}{(\xi^2-c^2)^2} g(\xi) + \frac{\xi}{\xi^2-c^2} g'(\xi)$$

where

$$g'(\xi) = 2\xi - \frac{\left[\sqrt{(\xi^2+c^2)^2 - 4R^2\xi^2} + \xi^2 + c^2\right] 8R^2\xi - 8R^2\xi^3 \left[\frac{\xi^2+c^2-2R^2}{\sqrt{(\xi^2+c^2)^2-4R^2\xi^2}} + 1\right]}{(\xi^2+c^2)^2 - 4R^2\xi^2 + (\xi^2+c^2)^2 + 2(\xi^2+c^2)\sqrt{(\xi^2+c^2)^2-4R^2\xi^2}}.$$

Also

$$f''(\xi) = \frac{2\xi(3c^2+\xi^2)}{(\xi^2-c^2)^3} g(\xi) - \frac{2(c^2+\xi^2)}{(\xi^2-c^2)^2} g'(\xi) + \frac{\xi}{\xi^2-c^2} g''(\xi)$$

and

$$f'''(\xi) = \frac{-6(\xi^4+c^4) - 34c^2\xi^2}{(\xi^2-c^2)^4} g(\xi) + \frac{6\xi(3c^2+\xi^2)}{(\xi^2-c^2)^3} g'(\xi)$$

$$- 3\frac{c^2+\xi^2}{(\xi^2-c^2)^2} g''(\xi) + \frac{\xi}{\xi^2-c^2} g'''(\xi).$$

It is easy to show that

$$g(0) = c^2$$

$$g'(0) = 0$$

and $$g''(0) = 2 - \frac{4R^2}{c^2} .$$

Therefore

$$f(0) = 0$$
$$f'(0) = -1$$
$$f''(0) = 0$$

and

$$f'''(0) = \frac{12}{c^2}\left(\frac{R^2}{c^2} - 1\right).$$

APPENDIX C

Suppose we wish to integrate $F(\zeta)$ in a circle of increasingly infinitesimal radius around a branch point, such as ζ_I in Fig. 10. It will be proved that this integral vanishes if

$$\lim_{\zeta \to \zeta_I} \left| (\zeta - \zeta_I) F(\zeta) \right| = 0.$$

Letting $\zeta = \zeta_I + \epsilon e^{i\theta}$:

$$\int_{ABC} F(\zeta)\, d\zeta = \lim_{\epsilon \to 0} \int_0^{2\pi} F(\zeta_I + \epsilon e^{i\theta})\, i\epsilon e^{i\theta}\, d\theta.$$

Hence

$$\left| \int_{ABC} F(\zeta)\, d\zeta \right| \leq \lim_{\epsilon \to 0} \int_C^{2\pi} |i|\, |\epsilon e^{i\theta} F(\zeta_I + \epsilon e^{i\theta})|\, d\theta$$

$$= \lim_{\zeta \to \zeta_I} \int_c^{2\pi} \left| (\zeta - \zeta_I) F(\zeta) \right| d\theta$$

$$\leq \lim_{\zeta \to \zeta_I} \left| (\zeta - \zeta_I) F(\zeta) \right|_{MAX} \cdot 2\pi$$

where ζ is that point on the circular contour which gives the maximum value indicated. Now if

$$\lim_{\zeta \to \zeta_I} \left| (\zeta - \zeta_I) F(\zeta) \right| = 0$$

for any mode of approach of ζ to ζ_I , then it is also true along the path of maximum absolute values. Hence

$$\int_{ABC} F(\zeta)\, d\zeta = 0$$

and the theorem is proved.

Unclassified

Security Classification

DOCUMENT CONTROL DATA - R & D

(Security classification of title, body of abstract and indexing annotation must be entered when the overall report is classified)

1. ORIGINATING ACTIVITY (Corporate author)
Boston University
110 Cummington Street
Boston, Massachusetts 02215

2a. REPORT SECURITY CLASSIFICATION
Unclassified

2b. GROUP

3. REPORT TITLE

VORTEX INDUCED ROLLING MOMENTS ON FINNED MISSILES AT HIGH ANGLE OF ATTACK

4. DESCRIPTIVE NOTES (Type of report and inclusive dates)
Scientific. Interim

5. AUTHOR(S) (First name, middle initial, last name)
Daniel G. Udelson

6. REPORT DATE	7a. TOTAL NO. OF PAGES	7b. NO. OF REFS
November 1968	54	16

8a. CONTRACT OR GRANT NO.	9a. ORIGINATOR'S REPORT NUMBER(S)
F19628-68-C-0148	Scientific Report No. 1
b. PROJECT NO. 7659-04-01	
c. Dod Element 62101F	9b. OTHER REPORT NO(S) (Any other numbers that may be assigned this report)
d. Dod Subelement 681000	AFCRL-68-0569

10. DISTRIBUTION STATEMENT

1 - Distribution of this document is unlimited. It may be released to the Clearinghouse, Department of Commerce, for sale to the general public.

11. SUPPLEMENTARY NOTES	12. SPONSORING MILITARY ACTIVITY
TECH, OTHER	Air Force Cambridge Research Laboratories (CRE) L. G. Hanscom Field Bedford, Massachusetts 01730

13. ABSTRACT

Previous analytical studies endeavoring to account for vortex induced rolling moments on missiles have not successfully correlated with experimental results. This points up the need for a theoretically more sophisticated treatment, which the present work attempts to satisfy.

A model for the two dimensional cross flow past the tail body combination is employed and the Blasius complex contour integral used to find the moments. The integral is solved by examining the singularities (poles and branch points) inside the contour.

This is the first scientific report in a continuing research effort. The final result contained herein presents the complete mathematical solution for the two dimensional ideal flow past a planar tail body combination. It is in closed analytic form with the exception of one definite integral which has been reduced to a form suitable for numerical calculation. All terms of the solution (integrated as well as the integral) are best calculated for various values of the parameters on a large scale digital computer.

DD FORM 1 NOV 65 1473

Unclassified

Security Classification

14. KEY WORDS	LINK A		LINK B		LINK C	
	ROLE	WT	ROLE	WT	ROLE	WT
Blasius Integral						
Finned Missiles						
Missiles						
Rolling Moment						
Vortex						